NATIONAL ACADEMY OF SCIENCES

Number 43 • January 1961

IGY BULLETIN

A monthly survey of programs and findings of the International Geophysical Year and the International Geophysical Cooperation–1959 as related primarily to United States programs. The Bulletin *also reports on international programs in geophysics and space science that have grown out of the IGY, and on their results.*

UNIVERSITY OF ILLINOIS LIBRARY CHICAGO

Meteorological Rockets and Satellites

The following is a summary of a paper by Harry Wexler, Director, Meteorological Research, U. S. Weather Bureau, presented at the Symposium on Space Research, Buenos Aires, Argentina, Nov. 28–Dec. 3, 1960.

The history of meteorology has been punctuated by a number of developments, notable among which have been the persistent efforts of meteorologists to observe ever larger portions of the atmosphere—with the ultimate goal of observing all five billion million tons of it. In recent years there has been marked progress toward this goal.

In exploring the atmosphere vertically, the meteorologist has made successive leaps upward using mountain observatories, manned balloons, kites, unmanned balloons, airplanes, radar, and rockets. He has extended his observing capability horizontally by establishing weather-station networks on land and, to a much less adequate degree, over oceans and polar regions. In recent years, the new technique of sounding the upper air with meteorological rockets has been made more effective by the development in the United States of a network of synoptic rocket-sounding stations, and now, for the first time, the meteorologist has access to an observing platform commensurate with the global scale of the atmosphere—the earth-orbiting satellite.

Rockets

Even before data from light-weight meteorological rockets became available, meteorological sounding balloons penetrating above the 25-kilometer level occasionally showed large temperature increases and changes in wind patterns during the winter at higher latitudes in the northern hemisphere. This "explosive warming," first noticed in February 1952 over Berlin, Germany, has since been observed in many areas of the northern hemisphere, particularly in the vicinity of northeast Canada during January and February. IGY meteorological rockets launched at Fort Churchill, Canada, to much greater heights than those reached by meteorological balloons showed that during such periods of explosive warming, winter temperatures in some air layers above 30 km rose to values higher than those observed in midsummer, while wind patterns changed from mostly zonal (east or west) to meridional (north or south).

(Figure 1 is a time section showing changes in temperature and in wind speed and direction above Fort Churchill for the month of August 1957. The figure indicates how rocket data helps fill in the picture for the region above 30 km. *Bulletin No. 40* contains a fuller report on rocket-grenade studies at Fort Churchill.)

This explosive warming, found nearly every year somewhere in the northern polar regions, is not observed to such a marked extent in the southern polar regions. Four years of observation at the IGY Amundsen-Scott South Pole Station reveals only one slight warming, of about 10°C in 24 hours,

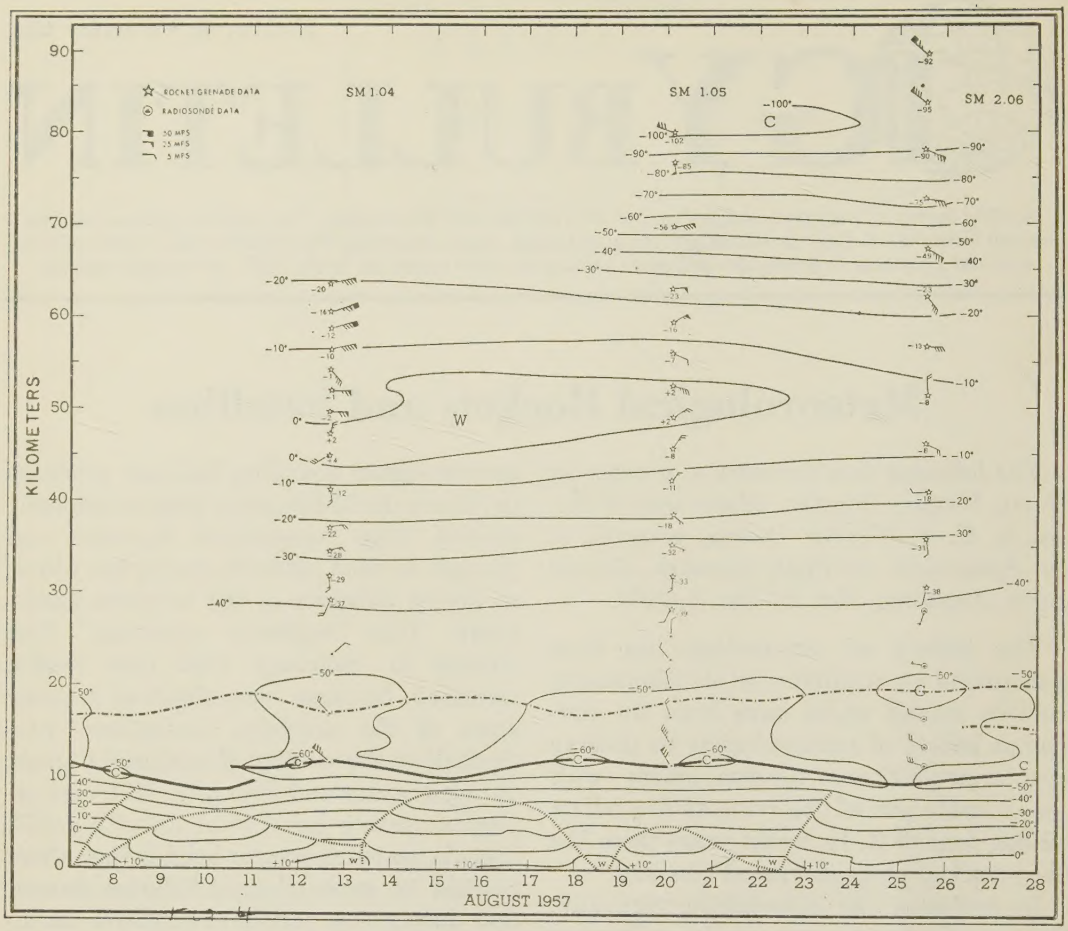

Fig. 1. *Time Section to a Height of 90 Kilometers above Fort Churchill, Canada, August 8–28, 1957. Wind and temperature data based on radiosonde measurements below 30 km and on rocket measurements above 30 km (temperatures in °C). Fronts shown by dotted lines, tropopause by heavy solid line, and thermal boundary by dash-dot line; C and W indicate cold and warm areas. Barbs representing wind speed are at tail end of wind shafts, which point in direction in which wind is blowing —with north at the top of the diagram and east to the right. (From a report by Sidney Teweles, US Weather Bureau.)*

in June 1960, at a pressure level of 40 millibars (20 km). For each of the four springs, 1957 through 1960, the major warming took place about one month after return of the sun above the horizon. This is in quite marked contrast to the pattern in the northern hemisphere, where the warming occurs most often during the polar night.

The spring warming in the south polar region cannot be attributed entirely to solar radiation since, in 1957 for example, the temperature again decreased after the first marked warming peak was reached (in early November) despite the fact that the sun's elevation was increasing; moreover, even at the summer solstice, the 50-mb temperature was 10°C lower than that observed six weeks earlier. The temperature changes in subsequent springs were not as marked as that in 1957, but still indicated that non-solar influences were important.

A completely satisfactory explanation has not yet been found for this remarkable difference between behavior of the northern and southern polar stratospheres. One possible explanation is that the much larger

west-east continental-oceanic contrast in the northern hemisphere exerts a strong influence on the high stratosphere, causing the intense polar cyclone that forms in the early winter to become perturbed and to split into a number of smaller anticyclonic and cyclonic vortices. The anticyclonic vortices are associated with descending air and the cyclonic vortices with rising air, both effects combining to produce a marked temperature gradient between the two types of vortices. If this geographic explanation is correct, meteorologists may have to revise their estimates as to how high in the atmosphere continental-oceanic influences extend.

Another possible explanation is that there is a feeding-in of extra-terrestrial energy unequally in the two hemispheres. Perhaps the Van Allen radiation belts (see *Bulletin Nos. 30* and *32*), which dip into the auroral zones of both hemispheres, may spill more energy into the northern polar regions than into the southern polar regions. However, the energies involved, estimated to be no more than 10 or 100 ergs/cm^2/sec at 100 km, are much too small to account *directly* for the temperature rises of as much as 45°C in 48 hours observed at 25-30 km. It is possible, of course, that even these slight inputs of energy may "trigger-off" changes in flow and in thermal patterns which themselves may induce larger temperature changes by means of vertical motions, but no satisfactory quantitative model for this type of reasoning has been proposed.

The northern hemisphere studies indicate that there is also a great need for lightweight meteorological rocket observations at high latitudes in the southern hemisphere to determine whether, above the ceiling of meteorological balloons, there may be found during the southern polar night the extreme thermal and wind unrest found in the northern polar regions.

Satellites

As always, when the meteorologist is able to observe the atmosphere in new ways he encounters new things. The more extensive the view the better organized the atmosphere appears to be. Phenomena that appear chaotic and random when seen by limited vision take on an orderliness when observed by satellite that holds promise of improved quantitative analysis and prediction. A meteorological satellite in a polar orbit can survey the earth's entire atmosphere twice a day. With an adequate number of such satellites, it should be possible to keep under continuous surveillance every portion of the atmosphere.

Because of the close association of cloud distribution with cyclones and anticyclones, cloud photography was the first objective of the United States meteorological satellite program. The first television cloud-observing satellite, TIROS I, launched April 1, 1960 (see *Bulletin No. 35*), produced nearly 23,000 pictures of the earth during its 78 days of useful life; more than 60% of these are good-quality cloud photographs, useful in meteorological research. The pictures yielded almost immediately two important findings: spiral cloud patterns with diameters as great as 1000 miles (*Bulletin No. 35*, Fig. 10), and large areas composed of many crescent- or doughnut-shaped cloud cells with diameters of 30 to 50 miles (Fig. 2).

Many of the large spiral cloud patterns have a marked banded structure and are associated with cyclonic storms. No two of these cyclonic cloud patterns are exactly alike. The smaller, 30- to 50-mile-wide, cellular clouds are apparently of convective origin and are too large to be seen by the human eye but too small to be recognized on conventional meteorological charts. These convective cells probably play an important role in transferring heat, water vapor, and momentum from the surface to the lower layers of the atmosphere.

TIROS I photographs also revealed other interesting meteorological and related phenomena, including cloud bands of a tropical cyclone north of New Zealand; cirrus streamers associated with the jet stream over the southern Andes; double-vortex

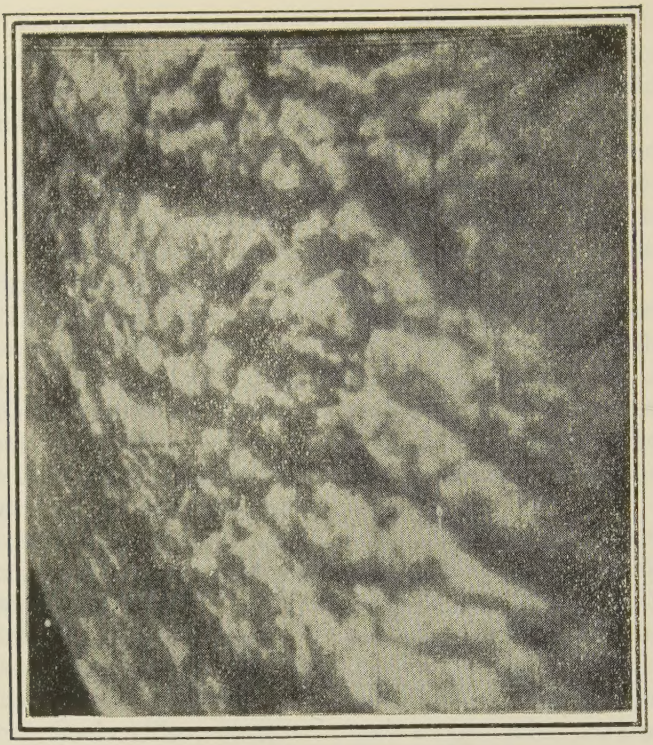

Fig. 2. *TIROS I Wide-angle Photograph of the Tropical South Pacific Showing "Cloud Streets" Consisting of Large Cumuliform Cloud Masses Representing Large Convective Cells. The clouds are embedded in the easterly tradewinds.*

clouds in cyclones apparently having only one low-pressure center; cumulus cloud "streets" in the tropics (Fig. 2); a single, long, thin cloud about five miles wide and several hundred miles long in the vicinity of the Gulf Stream east of Florida, and its reverse—a long, thin *cloudless* streak imbedded in an otherwise continuous cloud cover near Madagascar; a broken pattern of sea ice in the Gulf of St. Lawrence; and snow fields in the Himalaya Mountains and in the Alps. In addition, a series of photographs obtained from five orbits over the southern Indian Ocean in late April, 1960, enabled construction of a synoptic cloud chart for that area, composed of four main cyclonic centers. One of these storms later moved into southern Australia, giving a prolonged period of precipitation.

The successful TIROS I experiment clearly shows that meteorological satellites must be included as an integral part of a comprehensive world-wide weather observing system. Their ability to give complete global coverage, to look at familiar meteorological phenomena from a new vantage point and to reveal organized motions and processes over a great range of dimensions, will influence virtually all phases of meteorological development and operations.

TIROS II, launched on November 23, 1960, continues the cloud-cover experiment begun with TIROS I and, in addition, carries several infrared radiation sensors to measure the earth's heat balance, temperatures of cloud tops and of the earth's surface, and other properties. TIROS II is described elsewhere in this *Bulletin*.

Geology of the Windmill Islands, Antarctica

The following material is based on a report by Richard Robertson, of the Ohio State University Research Foundation. The original report was published by the Foundation in September, 1959, as USNC-IGY Antarctic Glaciological Data Report No. 2, Part IV, Preliminary Report of the Bedrock Geology of the Windmill Islands.

The Windmill Islands area is the most extensive area of exposed rocks in the coastal region of East Antarctica between the Bunger Hills, 250 miles to the west, and King George V Land, 1000 miles to the east. Capes and islets extend for about 20 miles along the eastern side of Vincennes Bay, where they are exposed at the margin of the continental ice sheet. (See *Bulletin No.* 32, Fig. 7.) Wilkes IGY Station is at 66° 15′ S, 110° 31′ E, at the western tip of Clark Island, near the northern end of the Windmill Islands (see Fig. 3).

Geologic field observations were made in 1958 by Richard Robertson, aided by Caspar Cronk and John Hollin; all were members of the Wilkes Station scientific staff. Geologic mapping was carried out using US Navy Hydrographic Office charts (scale 1:12,000) and other maps prepared in the field; final data were transferred to a topographic map at the scale of 1:50,000. This report is based on hand-specimen identification of the rocks. A detailed petrographic analysis of rocks from the Windmill Islands area is now in progress; the work is supported by the Institute of Polar Studies, Ohio State University.

(*Note: All or most of the rock nomenclature used in this report can be found in standard dictionaries.*)

Physiography

The topography of the Windmill Islands is relatively gentle and is controlled to some extent by the rock types present. Summits of the hills are generally accordant at an elevation of about 250 feet and may represent an old erosion surface. This surface is cut by "*U*"-shaped valleys formed by glacial activity and by broad, deeper valleys which, at present, form arms of the sea. The area below sea level has considerably greater topographic relief than that above. An especially good example of this difference in relief occurs south of the island group, where a 1000-fathom trench extends outward from the Vanderford Glacier; this trench may represent a fjord scoured out earlier by the glacier.

The southern islands are composed of igneous rocks in a stock-like or batholithic intrusion, and the northern islands consist of various metamorphic rocks with a migmatite zone in the region adjacent to the intrusion. (A stock is a body of igneous rock formed at great depth, generally granitoid in texture, and covering up to 40 square miles in surface area; similar but still larger bodies are termed batholiths. Migmatite is a layered or mixed rock of alternating pods or irregular zones of schist and granitic material.)

In general, the topography of the islands to the south is more rugged than that of the islands to the north. The Frazier Islets, however, which are the westernmost of the Windmill Islands and among the most northerly, have high, steep cliffs.

Water from melting snow is present for as much as three months of the year. This water occupies no well-defined bedrock channel but flows through ground moraine in wide, thin sheets. The ground moraine—scattered rock debris deposited from the bottom of melting glaciers—is concentrated in the flat-bottomed valleys. Where the melt water is especially abundant, small lakes form behind dams of permanent ice, morainal material, or sills of bedrock.

Vegetation is limited to mosses, lichens, and colonies of algae, which form thick carpets in moist, wind-sheltered areas. Ani-

mal life is restricted to Adelie penguins, petrels, skuas, a few seal species, and sea elephants.

Rock weathering is promoted largely by the freezing of water in fractures. This frost-wedging process goes on even when the air temperature is considerably below freezing since strong solar radiation warms the rocks sufficiently to cause a film of water to form, some of which seeps into cracks in the rocks and re-freezes. Prominent honeycomb rock surfaces are found on Browning and Peterson Islands. The honeycombing may start at breaks in a hard outer crust formed over deeply weathered rocks. These breaks in the outer crust allow the agents of physical weathering to create hollows in the less resistant material beneath the protective crust. Chemical weathering has penetrated to a depth of 20 inches in the igneous rocks and is elsewhere evidenced by copper and manganese stains, similar to desert varnish.

Rock Types

Five broad groups of igneous and metamorphic rocks are present in the Windmill Islands (see Fig. 3). They are, in order of probable decreasing age: metamorphic rocks —locally migmatites; amphibolite dikes and pods; acidic (more than 66% SiO_2) to intermediate (52 to 66% SiO_2) porphyritic intrusive (containing large crystals in a finer-grained groundmass) igneous rocks; porphyritic foliated granite (with phenocrysts—or larger crystals—in a sub-parallel orientation and consisting of potassium feldspar); and basaltic to gabbroic dikes—tabular bodies of igneous rock intruded across the structure of the bedrock.

The gneiss, schist, and migmatite making up the metamorphic rocks are commonly composed of biotite, feldspar, and quartz. Garnet and magnetite, and locally pyroxene and amphibole, are accessory minerals in the metamorphic rocks. Foliation of these rocks is regular, and crenulations, or small folds, are widely separated everywhere except on Frazier and Chappel Islands, where the gneiss is finely crenulated.

Amphibolite pods cutting across the metamorphic rocks are thought to be altered basaltic dikes, and an intrusive body of amphibolite is exposed on Robinson Ridge, at the margin of the stock, or batholith.

The porphyritic rocks of this massive intrusive body are varied in texture and, in general, they are more coarsely crystalline to the west. The composition ranges from that of granite to that of quartz diorite. Bodies of older rocks included within the stock, or batholite, are not common, but Boffa Islet is made up of a jumbled mass of such inclusions. Ford and Cloyd Islands are composed of foliated porphyritic granite in tabular bodies that may be younger than the surrounding stock.

Dikes of diabase, gabbro, and diorite cutting through all of the older rocks form a sub-parallel system in the Bailey-Mitchell Island area along the crest of an anticlinal (upwarped) fold in the bedrock. Similar dikes also intrude the stock in the Odbert and Browning-Peterson Island area.

Bedrock Structure

Asymmetrical anticlinal and synclinal (downwarped) folds, trending approximately NW-SE, have been identified in the migmatite of the northern islands. (In an asymmetric fold, one limb dips more steeply than the other.) The syncline is north of Clark Island and the anticline is between Bailey and Mitchell Islands. The distance between crests of the two folds is about 10,000 feet and they both plunge toward the SE. (Plunge is the dip of the axis of the fold below the horizontal.) The southernmost limb of the anticlinal fold is truncated by a stock (see profile in Fig. 3).

The general shape of the synclinal fold is probably similar to that of the many smaller folds on Clark Island, just south of it. These small folds are generally parallel, eastward-plunging, and isoclinal (limbs parallel) in most places, but some plunge in both directions. One small fold on Clark Island has an axial fault of small displacement.

The large anticlinal fold between Bailey

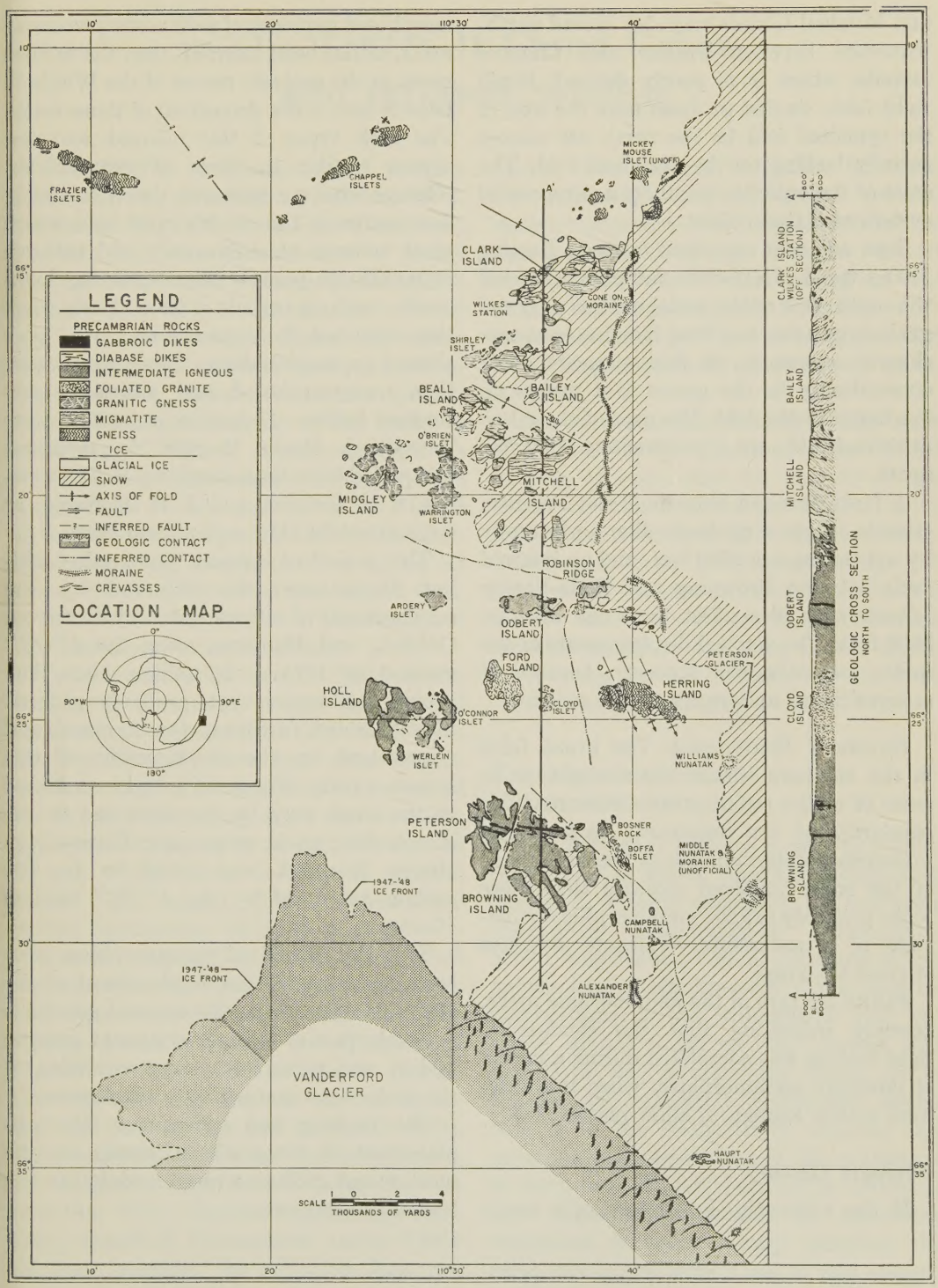

Fig. 3. *Geologic Map of the Windmill Islands. At right is profile along line AA'. (Adapted from map compiled by R. Robertson, drafted by G. A. Van Niel, and based on US Navy Hydrographic Office Map 6669 [1959], corrected by field observations and aerial photographs.)*

and Mitchell Islands may also extend northwestward between Frazier and Chappel Islands, where it is poorly defined. Small tight folds similar to those near the axis of the synclinal fold to the north are almost entirely lacking on the anticlinal fold. The crest of the anticline is cut by a sub-parallel system of diabase dikes.

Two adjacent anticlinal folds on Herring Island trend NNW-SSE and plunge toward the south. One of the anticlines has a core of gneissic granite, and long boudins (sausage-shaped segments) of this material occur concordantly in the gneiss that makes up the flanks of the fold. The axes of these two anticlinal folds are approximately 5000 feet apart.

A fault between Browning and Peterson Islands offsets a gabbroic dike horizontally by approximately 2000 feet, and an inferred fault between Browning and Boffa-Bosner Islands may also offset the same dike by 5000 feet. The vertical displacements of the faults are unknown, however, because of compositional uniformity of the stock.

Structural Development: The broad folds in the northern islands are thought to be relics of earlier sedimentary structures. The regularity of the structural pattern and preliminary determination of the mineralogy of the rocks involved indicate that these rocks probably are the metamorphic equivalents of a sedimentary-volcanic sequence of great thickness.

Faults are rare in the metamorphic rocks, possibly indicating that the small-scale, tight folding was completed during a period of intensive metamorphism when the rocks were mobile enough to allow plastic flow.

Geologic History

If the migmatite is an intensely metamorphosed sequence of sedimentary-volcanic rocks, as has been inferred, then the earliest event in the geologic record of the Windmill Islands area is the deposition of those rocks. The rock types of this inferred sequence appear similar to those of geosynclines. (Geosynclines are extensive, slowly subsiding downwarps in the earth's crust into which great volumes of sedimentary and volcanic materials are poured from bordering highlands over long periods of time.) Basic dikes then intruded the sequence and were later altered to amphibolites. These rocks were then metamorphosed and extensive concordant bodies of alaskite pegmatite were introduced. Rocks thought to represent this period have been dated, by R. L. Cameron, S. S. Goldich, and J. H. Hoffman, at approximately 1115 $\pm$ 5 million years.

This period of orogeny (mountain-building disturbance) was followed by the emplacement of a stock dated by Cameron, Goldich, and Hoffman, using the A^{40}/K^{40} method, at 1075 $\pm$ 25 million years. The geosynclinal sequence was probably rendered plastic, folded, further metamorphosed, and migmatized by the emplacement of this adjacent body. The granite body contained in the stock may be the same age as the surrounding stock, or younger. Gneiss from Haupt Nunatak was found to be 960 million years old by the A^{40}/K^{40} method (Cameron, et al.)

This last period of metamorphism may have accompanied the emplacement of the granitic bodies. If so, the exposed granite is probably part of a larger system of granitic bodies, and some further reconstitution of the rocks accompanied their emplacement.

The faulting and subsequent dike emplacement in the southern islands are the most recent geologic events recorded in the bedrock of the area.

The TIROS II Cloud-Cover and Infrared Satellite

The TIROS II meteorological satellite (1960 Pi) was launched at 6:13 am EST, November 23, 1960, from Cape Canaveral, Florida, and was injected into a nearly circular orbit 13 minutes later. The satellite's primary instrumentation consists of two television cameras, to photograph the earth's cloud cover, and sensors to map solar and infrared, or heat, radiation in various spectral bands. With the exception of the radiation equipment, TIROS II closely resembles the TIROS I satellite, launched on April 1, 1960 (see *Bulletin No. 35*), and like that of TIROS I, the TIROS II experimental instrumentation is expected to remain in operation for about three months from the launch date. ("TIROS" is a contraction of Television and Infrared Observation Satellite.)

The launch vehicle was a Delta rocket similar to that used to put the Echo I communications satellite into orbit (see *Bulletin No. 39*). Five days after launch, the following orbital elements were released for TIROS II: apogee, 453.2 statute miles; perigee, 386.9 statute miles; velocity at apogee, 16,689 mph; velocity at perigee, 16,943 mph; period, 98.37 minutes; and orbital inclination, 48.53°.

Over-all responsibility for the TIROS project rests with the National Aeronautics and Space Administration, and the operational phase is under the direction of NASA's Goddard Space Flight Center. The radiation experiments were designed, and the data storage and telemetry equipment associated with them were constructed, by Goddard, which is also analyzing the radiation data. Barnes Engineering Company, Stamford, Connecticut, under NASA contract, provided the radiation detectors. Except for the radiation experiments, the satellite was designed and constructed by the Astro-Electronics Division of the Radio Corporation of America, Princeton, New Jersey, under contract to NASA. RCA was also responsible for the special ground-station equipment. The Delta launch vehicle was constructed by the Douglas Aircraft Corporation, which also conducted the launch. Other participants in the development and construction of the payload, and in tracking operations, are the same as for TIROS I.

The Meteorological Satellite Laboratory of the US Weather Bureau, under NASA funding, is responsible for analysis of the cloud-cover data and will participate in the processing and analysis of the radiation data. Cooperating in the project are various Department of Defense agencies. The Weather Bureau and the military weather services are attempting to use some of the cloud-cover data for a limited, experimental, operational analysis program.

Experimental Aims and Instrumentation

The TIROS II satellite is part of a long-range United States program designed to develop a satellite capability for providing world-wide meteorological information. Three major aims behind development of meteorological satellites are: (1) to produce observations of the atmosphere over the entire globe, including the oceans and deserts as well as inhabited areas; (2) to provide as completely continuous observations as are scientifically required and technologically possible; and (3) to attempt to learn how the sun's energy is converted into atmospheric motions by measuring variations in solar energy reaching the earth and in the earth's use of this energy.

TIROS I demonstrated the feasibility of meteorological satellites. It transmitted 22,952 cloud-cover photos during its operating lifetime of nearly three months, relaying

to ground stations meteorological information from many regions of the world where weather information had previously been scanty or entirely lacking and providing new information on patterns of atmospheric circulation and on cloud formations. Some results of analyses of TIROS I cloud photographs have already appeared in the literature[2,3,4,5,6,7,10, and 11].

TIROS II continues the cloud-cover experiment of TIROS I using identical wide- and narrow-angle television cameras[1,8,9, and 12] that "look" through the baseplate of the satellite (*Bulletin No. 35*). Power and telemetry equipment associated with this experiment are also similar to those of TIROS I. In addition, both satellites were equipped with infrared horizon sensors to help determine the satellites' attitude in space and with special solar cells to measure the satellites' position with respect to the sun, permitting calculation of the north direction for use in interpreting cloud-cover data.

The major differences between the instrumentation of the two satellites are in the addition of the infrared equipment in TIROS II and of magnetic instrumentation to control the orientation of TIROS II's spin axis. The infrared and magnetic-orientation-control equipment are described below.

Radiation Experiments: TIROS II carries two radiation experiments[8,9,12]. One consists of five radiation detectors, oriented at 45° to the spin axis, which scan through a combination of the satellite's rotation and its movement along the orbit. These detectors measure:

(1) The earth's albedo—the percentage of reflectivity of radiant energy, or light—in the spectral range 0.2-5 microns.

(2) Infrared radiation emitted by the earth and atmosphere combined in the range 7-30+ microns.

(3) Emitted infrared radiation coming through the atmospheric "window" (the portion of the electromagnetic spectrum to which the atmosphere is quite "transparent") in the range 8-12 microns. Measurements in this spectral range should supply information that may permit (a) cloud detection, especially at night and over areas where the TV cameras are not operated; (b) determination of cloud-top temperatures and, accordingly, a rough measure of cloud-top height; and (c) determination of surface temperatures over cloud-free areas.

(4) Radiation from the water-vapor spectral band, 6.3 microns ± 5%. These measurements should show the geographic distribution of the approximate upper margin of water vapor in the atmosphere, which, in some places, may be near the height of the tropopause (about 20,000–50,000 feet above sea level).

(5) Visible radiation in the spectral range 0.5-0.7 microns. This visual channel is intended to provide maps of visible radiation for use in relating the television pictures and the nonvisible-radiation maps.

The second radiation experiment consists of two sensors, one white and the other black, which together measure the heat balance of the portions of the earth's surface and atmosphere viewed by the wide-angle television camera. The white sensor measures heat radiation from the earth while the black sensor measures both visible (reflected solar radiation) and heat radiation.

Data from the radiation experiments are recorded continuously for each orbit on magnetic tape, to be played back over a three-watt, 237.8 mc/sec transmitter on command from one of the ground stations. If not read off after one orbit, the tape automatically starts erasing its previous data as it begins recording during the next orbit. However, the tape always has the last 100 minutes of radiation data stored on it for playback whenever commanded.

Magnetic Orientation Control: A satellite spinning in space can develop a dipole magnetic field similar to that of a small bar magnet as a result of closed current loops in the circuitry and of any magnetic materials

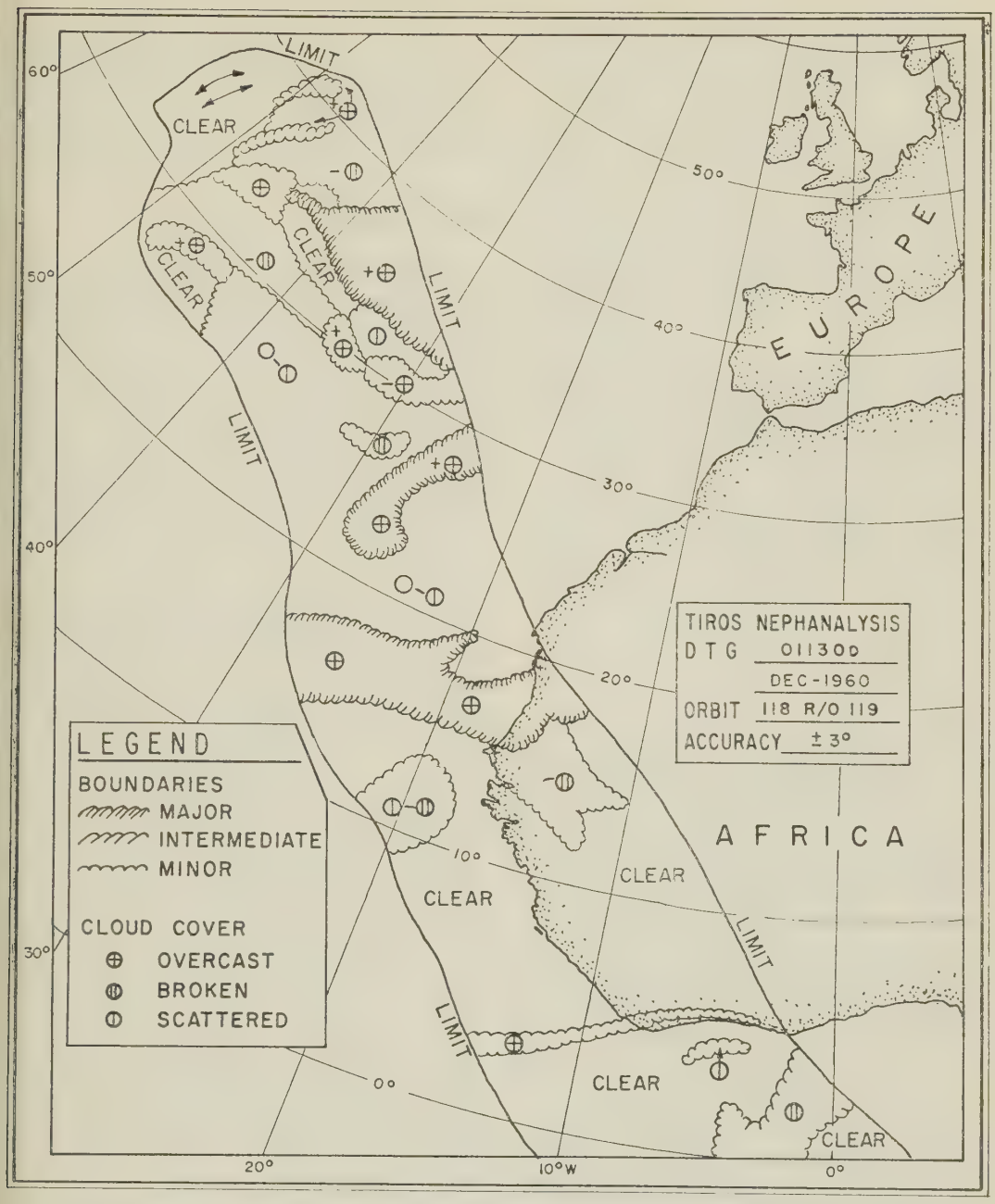

Fig. 4. *Nephanalysis of a Portion of TIROS II's 118th Orbit, on December 1, 1960, Over the North Atlantic and Western Africa. Plus (+) and minus (−) signs indicate relative density of cloud cover; DTG Signifies "Date-Time Group." Arrows represent streaky cloud structure. (From US Weather Bureau.)*

present in the satellite. The magnetic dipole, interacting with the earth's magnetic field as the satellite orbits, produces a torque—or turning force—which slowly changes the direction of the satellite's spin axis in space, thus also changing the direction in which the television cameras are pointing. This effect was discovered in TIROS I.

It was believed that the strength of the magnetic dipole and, therefore, changes in the spin-axis direction, could be controlled to some extent by programming, by ground command, various steady currents through a coil of wire wound around the outside of the satellite. An experiment to test this thesis was incorporated in TIROS II, and, to date, the coil has been activated successfully three times in efforts to change the orientation of the spin axis in order to obtain better performance from the television and radiation-measuring systems. The apparatus consists of an aluminum wire wound around the sides of the satellite just above the baseplate. Current from the satellite's power supply is fed through this coil by command from the ground. The current can be turned on or off, or varied in both direction and magnitude, when the satellite is under control of one of the ground stations.

Spin Control

When separated from the third stage of the Delta launch vehicle, TIROS II was spinning at a rate of about 126 rpm. About 10 minutes later, a timer released a de-spin mechanism, consisting of two weights attached to cables wound around the satellite, slowing the revolutions to about 8 rpm. To remain stable in orbit, however, the satellite must maintain a spin rate of at least 9 rpm. Thus, on the morning of November 25, 1960, one of five pairs of control rockets located around the satellite's baseplate were fired by ground command, speeding up the rotation to 10.8 rpm.

Later in the same day, it was noted that the satellite's spin axis was still precessing, or wobbling, slightly. To compensate for this precession, another pair of spin-up rockets was fired, raising the spin-rate to 13.9 rpm, which appeared to be keeping precession within tolerable limits.

Ground Stations

The two primary ground-command and data-read-out stations for TIROS II are located at San Nicolas Island, California (part of the Pacific Missile Range), and at Fort Monmouth, New Jersey. A backup station is located at Princeton, New Jersey.

First Results

Good-quality data have been obtained from the narrow-angle camera and from the infrared experiments since the launching of TIROS II. Pictures from the wide-angle camera, however, have not generally been as high in quality as those obtained by TIROS I, although the quality is good enough to permit meteorologists at the two data-read-out stations to prepare broad-scale cloud analyses on an experimental, real-time basis.

Figure 4 is an example of the schematic depiction of TIROS II cloud observations over the North Atlantic and part of Africa on orbit 118, December 1, 1960. The system used in this cloud-analysis (or nephanalysis) depiction was developed by the Weather Bureau on the basis of experience with photographic data from TIROS I. It is designed to present, in a simple graphical form suitable for transmission on national facsimile circuits, that portion of the available cloud-cover information likely to be of greatest general usefulness.

To assist users of the satellite cloud-cover data, the Weather Bureau's Office of Forecast Development issued, in December 1960, its Forecast Development Report No. 1, *Depiction of Satellite Cloud Observations for Facsimile Transmission.*

Participation by Other Countries

Immediately after the launching of TIROS II, the Space Science Board (SSB) of the US National Academy of Sciences sent to the Committee on Space Research (COSPAR), in The Hague, a telegram giving orbital and instrumental details of the satellite for transmittal to all COSPAR

participants. Data obtained by TIROS II will be deposited in the World Data Center A meteorological subcenter, at Asheville, North Carolina. When copies are available, notification will be sent to participants through COSPAR.

Prior to the launching of TIROS II, NASA and the US Weather Bureau invited weather agencies in a number of other countries to participate in meteorological research connected with the TIROS experiment. It was suggested that such weather agencies might wish to intensify their standard meteorological observations or conduct special observations during passes of the satellite.

Weather agencies of several countries have been taking part in the experiment. NASA is providing orbital information to assist cooperating groups in these countries in timing local weather observations. After processing, TIROS cloud-cover photos will be forwarded to foreign participants for comparison with their supplementary observations; infrared data will also be forwarded to these participants.

Note: The US Weather Bureau suggests that, since the wide-angle camera in TIROS II has not performed as well as expected, weather agencies desiring to participate in the TIROS experiment may wish to plan their special programs in conjunction with TIROS III, which is expected to be launched later in 1961.

References

1. Johnson, D. S.: Image Sensing as Applied to Meteorological Satellites. *Journal of the Society of Motion Picture and Television Engineers.* Vol. 69, pp. 14–18. January 1960.
2. D. Q. Wark and R. W. Popham: TIROS I Observations of Ice in the Gulf of St. Lawrence. *Monthly Weather Review.* Vol. 88, no. 5. pp. 182–186. May 1960.
3. H. Wexler and S. Fritz: TIROS Reveals Cloud Formations. *Science.* Vol. 131, no. 3415. pp. 1708–1710. June 10, 1960.
4. S. Fritz: Cyclone Prints From Satellite TIROS I. *Interavia.* Vol. XV, pp. 1384–1385. November 11, 1960.
5. J. Winston: Satellite Pictures of a Cut-off Cyclone over the Eastern Pacific. *Monthly Weather Review.* September–December 1960.
6. C. Bristor and M. Ruzecki: TIROS I Photographs of the Midwest Storm of April 1, 1960. *Monthly Weather Review.* September–December 1960.
7. W. K. Widger, Jr.: Examples of Project TIROS Data and Their Practical Meteorological Use. *GRD Research Notes.* No. 38. July 1960. (Geophysics Research Directorate, AFRD, USAF, Bedford, Massachusetts.)
8. *Astronautics.* Vol. 5, no. 6. June 1960. pp. 32–45. (Collection of reports describing ground equipment and payload instrumentation of TIROS satellites.)
9. Hearings before NASA Authorization Subcommittee of the Committee on Aeronautical and Space Science, U. S. Senate, Second Session on H. R. 10809. March 28–30, 1960.
10. TIROS I—*TV* Weather Eye in Space. *Weather Bureau Topics.* Vol. 19. pp. 45–47. March, 1960.
11. W. G. Stroud: Initial Results of the TIROS I Meteorological Satellite. *Journal of Geophysical Research.* Vol. 65, no. 5. May 1960. pp. 1643–44.
12. R. A. Hanel and W. G. Stroud: Infrared Imaging from Satellites. *Journal of the Society of Motion Picture and Television Engineers.* Vol. 69, no. 1. pp. 25–26. January 1960.

World Warning Agency Report

July 1-September 30, 1960

This report is one of a series issued periodically during and following the IGY and IGC-59 periods. The reports summarize, on a quarterly basis, solar-terrestrial activity and related decisions of the World Warning Agency (AGIWARN), which was established as part of the IGY World Days Program. The present report covers the third quarter of 1960. A report on the previous two quarters appeared in *Bulletin No. 41.*

Six major solar flares (classified 3 or 3+ by at least one observatory) were reported to AGIWARN during the third quarter of 1960. Of 12 geomagnetic storms recorded during this interval, World-wide Geophysical Alerts (see *Bulletin No. 23*) were issued for

all except two very minor disturbances on July 3 and August 8. No Advance Alerts were issued by the World Warning Agency in connection with the storm that commenced suddenly on August 16 or for the brief disturbance on September 2. All other storms were announced with Advance Alerts as soon as they were recognized as actual disturbances.

As in the last quarter, the magnetic disturbances were divided almost equally between the sudden-commencement type and the gradual-commencement type. Such a division is to be expected during a post-maximum phase of the sunspot cycle, as is now under way. This characteristic mixture of storm types, however, makes accurate forecasting extremely difficult.

Disturbed radio conditions lasting through a whole day were associated with six of the geomagnetic storms recorded, and the North Atlantic Radio Warning Service (NARWS) gave advance warning of three of these, including the most severe storm of the quarter, which began on September 4. All together, NARWS predicted four storms in advance—three on the basis of prior observation of "event-type" solar activity (i.e., having well-defined, observable beginnings and endings, and of short duration) and the other on the basis of the tendency of some solar-terrestrial phenomena to recur at 27-day intervals corresponding to the rotation period of the sun.

As recurrent patterns of solar-terrestrial activity become more clearly defined with the approach of the solar minimum, and if the large majority of geomagnetic storms fall within these patterns, as is usually the case, forecasts will again become more certain. AGIWARN notes that until that time in the present cycle, however, solar observatories have the opportunity of discovering new event-type sun-earth relationships and of exploring avenues of theoretical and statistical research that might lead to applicable prediction techniques.

The following is a list of major solar flares, geomagnetic disturbances, World-wide Geophysical Alerts, and Special World Intervals (SWI) for the quarter beginning on July 1 and ending on September 30, 1960:

Jul	3	15xx*	Magnetic storm begins
	6	05xx	Magnetic storm ends
	14	1702	Severe magnetic storm begins
	15	1600	Alert issued**
	17	10xx	Severe magnetic storm ends
	19	04xx	Magnetic storm begins
		1600	Alert issued
	20	04xx	Magnetic storm ends
	29	17xx	Magnetic storm begins
	31	1600	Alert issued
Aug	1	14xx	Magnetic storm ends
	8	13xx	Magnetic storm begins
	9	12xx	Magnetic storm ends
	11	1916	Class 3+ flare, S-SWF†
	14	0534	Class 3 flare; S-SWF
	16	1410	Magnetic storm begins
		1600	Alert issued
			SWI starts††
	18	11xx	Magnetic storm ends
			SWI finishes
	19	1615	Magnetic storm begins
	20	1600	Alert issued
	22	06xx	Magnetic storm ends
	29	0020	Magnetic storm begins
		1600	Alert issued
	30	1600	Alert issued; aurora expected
	31	11xx	Magnetic storm ends
Sep	2	0706	Class 3 flare; S-SWF
		17xx	Magnetic storm begins
		2234	Class 3 flare; S-SWF
	3	0037	Class 3 flare; Slow S-SWF†
		09xx	Magnetic storm ends
		1600	Alert issued
	4	0230	Severe magnetic storm begins
		1600	Alert issued
			SWI starts
	6	13xx	Severe magnetic storm ends
			SWI finishes
	25	0759	Class 3 flare

* "xx" indicates gradual beginning or ending of a disturbance, following the hour indicated, such that the precise moment could not be determined.

** No ending times for Alerts are issued, as was done during the IGY; this is now left to the discretion of individual observatories.

† Symbols for ionospheric effects are defined as follows: S-SWF—sudden short-wave fadeout and gradual recovery; Slow S-SWF—slow short-wave fadeout (taking 5–15 minutes) and gradual recovery.

†† SWI's, when warranted, start at the time the associated Alert is issued; they finish at the end of the day indicated.

A Very Large Recent Solar Flare

M. A. Ellison, Susan M. P. McKenna, and J. H. Reid, of the Dublin Institute for

Advanced Studies, report that the class 3+ flare of June 1, 1960 (see *Bulletin No. 41*), appears to have been one of the largest in recent years. Their report, in the September 10, 1960, issue of *Nature*, is based primarily on an analysis of Hα film records from the Lyot heliograph at the Royal Observatory, Cape of Good Hope; a complete photographic record of the flare at one-minute intervals was obtained under cloudless conditions.

At the time of maximum extent, the June 1 flare occupied an area of 46 square degrees, or 2230 millionths, of the sun's visible hemisphere (1 millionth = 1,170,000 square miles). Thus, this flare was comparable in area to the great flare of July 25, 1946, which covered an area of 2500 millionths of the solar hemisphere and occurred in association with one of the six largest sunspot groups observed between 1874 and 1954. (Data on the flare and sunspot group of July 1946 from M. A. Ellison, 1946 and 1955.)

IGY Bibliographic Notes

The following bibliographic references relating to IGY and IGC-1959 programs and findings were selected from a bibliography under preparation in the Science and Technology Division of the Library of Congress.

A. Aboud, W. E. Behring, and W. A. Rense: Emission-Line Intensities in the Solar Ultraviolet. *The Astrophysical Journal.* Vol. 130., no. 2. Sept. 1959. Pp. 381–383.

Approximate Positions of Artifical Satellites Obtained with the Baker-Nunn Schmidt Camera (1). *Tokyo Astronomy Bulletin,* Second Series, No. 118. Aug. 20, 1959. Pp. 1367–1380.

R. L. F. Boyd: Photography in the International Geophysical Year. *Nature.* Vol. 184, no. 4692, Oct. 3, 1959.

R. Cadiergues: De la Terre Adélie au Sahara: *Industries Thermiques* (Paris). Vol. 5, no. 6. June 1959. Pp. 291–295. Illus., diagr., map.

Calendar of Outstanding Geomagnetic Occurrences and Chromospheric Solar Flares. *U.R.S.I. Information Bulletin.* No. 113. Jan.-Feb. 1959. Pp. 57–63. Illus.

M. H. Cohen: Linear Polarization in Type III Bursts. *The Astrophysical Journal.* Vol. 130, no. 1. July 1959. Pp. 221–227. Diagr. illus.

Committee on Space Research. Draft Report On First Meeting, London. November 14-15, 1959. *U.R.S.I. Information Bulletin.* No. 113. Jan.-Feb. 1959. Pp. 94–106.

A. E. Covington: Internal Precision of the Daily Radio Flux Observations at 10.7 Centimetres. *Journal of the Royal Astrophysical Society* Canada. Vol. 53, no. 4. Aug. 1959. Pp. 156–161. Diagr.

E. P. Fedorov: On the Computation of the Pole Coordinates. *Bulletin Géodésique* (Paris). No. 54 Dec. 1, 1959. Pp. 29–34.

Jesús Abarca Figueroa: El Macrosismo Del 28 de Julio de 1957. *Anales Instituto de Geofísica* U.N.A.M. Cudid University (Mexico, D. F.). Vol. 3. 1957. Pp. 55–88. Illus., diagr., maps. (with English summary).

Jacques Gilbert, Bernard Valtat, and René Garcia: Calcul théorique de l'altitude de la station Charcot (Terre Adélie). *Comptes rendus hebdomadaires des séances de l'académie des sciences* (Paris). Vol. 249, no. 5. Aug. 3, 1959. Pp. 731–733.

T. Hatherton and G. G. Midwinter: Diurnal Variation of Aurora and Geomagnetic Disturbances at New Zealand Antarctic Stations. *Nature.* Vol. 184, no. 4690. Sept. 19, 1959. Pp. 889–890. Diagr.

Masaaki Huruhata, Tsuyoshi Nakamura, and Hiroyoshi Tanabe: Scanning Photoelectric Photometer and Method of Observation of Night Airglow for the International Geophysical Year. *Tokyo Astrophysical Bulletin.* Second Series, No. 94. Feb. 20, 1957. Pp. 1005–1010. Illus., diagr.

Yukio Kawabata: Geophysical Effects Associated with the High-Altitude Nuclear Explosion. Part V. Acoustic and Seismic Waves. *Journal of Geomagnetism and Geoelectricity.* Vol. 11, no. 2. 1959. Pp. 60–62. Diagr., illus., map.

R. W. Knecht: Observations of the Ionosphere Over the South Geographic Pole. *Journal of Geophysical Research.* Vol. 64, no. 9. Sept. 1959, Pp. 1243–1250. Diagr., refs.

Hiroshi Maeda: Geophysical Effects Associated with the High-Altitude Nuclear Explosion. Part I. Geomagnetic Disturbances. *Journal of Geo-*

magnetism and Geoelectricity. Vol. 11, no. 2. 1959. Pp. 42–47. Diagr. (Published also in *Journal of Geophysical Research*. Vol. 64, 1959.).

Peter M. Millman: The I.G.Y. Visual Meteor Programme—Progress Report No. 3. *Journal of Royal Astronomy Society*. Canada. Vol. 53, no. 3. June 1959. Pp. 137–141.

Charles S. Mullin, Jr., and H. J. M. Connery: Psychological Study at an Antarctic IGY Station. *U. S. Armed Forces Medical Journal*. Vol. 10, no. 3. March 1959. Pp. 290–296.

Tatsuzo Obayashi: Geophysical Effects Associated with the High-Altitude Nuclear Explosion. Part III. Ionospheric Radio Propagation Disturbances. *Journal of Geomagnetism and Geoelectricity*. Vol. 11, no. 2. 1959. Pp. 51–53. Illus., diagr. (Published also in *Nature*. Vol. 183. May 1959).

K. W. Ogilvie and M. M. Winn: Evidence for Cosmic Ray Energy Spectrum Changes During a Forbush Decrease. *Nature*. Vol. 184, no. 4690. Sept. 19, 1959. P. 888. Diagr.

H. P. Pogosjan: Seasonal Peculiarities of the Temperature and Atmospheric Circulation Regimes in the Arctic and Antarctic. *World Meteorological Organization* (Geneva). *Technical Note No. 28*. 1959. 20 p., Diagr. (WMO-No. 90. TP. 37) (with French, Russian, and Spanish summaries).

Kuniji Saito, Keizo Nishi, Tomoyoshi Kurashige, and Sumio Kobane: Air-Borne Sun-Pointing Device and its Test at the Annular Eclipse on April 19, 1958. *Tokyo Astronomy Bulletin*. Second Series, no. 112. Nov. 20, 1958. Pp. 1205–1214. Diagr., illus.

Edouard Selzer: Enregistrements simultanés en France, á l'équateur et dans l'Antarctique, des effets magnétiques lengendrés par l' "Expérience Argus". *Comptes rendus hebdomadaires des séances de l'académie des sciences* (Paris). Vol. 249., no. 13, Sept. 28, 1959. Pp. 1133–1135.

W. G. Stroud, W. Nordberg, W. R. Bandeen, F. L. Bartman, and P. Titus: Rocket-Grenade Observation of Atmospheric Heating in the Arctic. *Journal of Geophysical Research*. Vol. 64, no. 9. Sept. 1959. Pp. 1342–1343. Diagr.

William Thompson: Rilevamento preciso delle traiettorie di satelliti. *Missili* (Rome). Vol. 1, no. 2. Apr. 1959. Pp. 37–53. Illus., diagr.

G. K. Tushinsky, ed.: *Information Bulletin on IGY Activities of the Geographical Faculty of Moscow University*. Nos. 1–3. Moscow. 1958. (In Russian)

U. R. S. I.-A. G. I. Committee. Edinburgh Meeting, 21st-23rd July, 1958. *U.R.S.I. Information Bulletin*. No. 111. Sept.-Oct. 1958. Pp. 24–44.

Universidad Mayor de San Andres. Laboratoria de Física Cósmica, La Paz, Boliva: *Resumen De Labores—AÑO 1956–1957*. Sept. 1957. Pp. 13–19. Diagr.; *AÑO 1958*. Dec. 1958. Pp. 15–20, 24. Illus., diagr.

Hiroyuki Uyeda, H. Maeda, A. Kimpara, T. Obayashi, Saburo Ishikawa, and Y. Kawabata: Geophysical Effects Associated with the High-Altitude Nuclear Explosion. *Journal of Geomagnetism and Geoelectricity*. Vol. 11, no. 2. 1959. Pp. 39–41, 62–63. Map.

J. Van Mieghem: Antarctic Meteorology. *WMO Bulletin*. Vol. 8, no. 2. Apr. 1959. Pp. 61–67. Maps.

E. H. Vestine: Note on Conjugate Points of Geomagnetic Field Lines for Some Selected Auroral and Whistler Stations of the IGY. *Journal of Geophysical Research*. Vol. 64, no. 10. Oct. 1959. Pp. 1411–1414. Tables, refs.

Gilbert Weill: Aurores polaires et phénomènes crépusculaires observés en radiation 3914 Å dans l'Antarctique. *Comptes rendus hebdomadaires des séances de l'académie des sciences* (Paris). Vol. 249, no. 20. Nov. 16, 1959. Pp. 2092–2094. Diagr.

G. P. Woollard: Crustal Structure From Gravity and Seismic Measurements. *Journal of Geophysical Research*. Vol. 64, no. 10. Oct. 1959. Pp. 1521–1544. Diagr., refs.

Preprinted from *Transactions, American Geophysical Union*, Vol. 42, No. 1, March, 1961